Flexible Split-Ring Electrode for Insect Flight Biasing Using Multisite Neural Stimulation

Wei Mong Tsang, *Member, IEEE*, Alice L. Stone, Zane N. Aldworth, John G. Hildebrand, Tom L. Daniel, Akintunde Ibitayo Akinwande, *Fellow, IEEE*, and Joel Voldman*, *Member, IEEE*

***Abstract*—We describe a flexible multisite microelectrode for insect flight biasing using neural stimulation. The electrode is made of two layers of polyimide (PI) with gold sandwiched in between in a split-ring geometry. The split-ring design in conjunction with the flexibility of the PI allows for a simple insertion process and provides good attachment between the electrode and ventral nerve cord of the insect. Stimulation sites are located at the ends of protruding tips that are circularly distributed inside the split-ring structure. These protruding tips penetrate into the connective tissue surrounding the nerve cord. We have been able to insert the electrode into pupae of the giant sphinx moth *Manduca sexta* as early as seven days before the adult moth emerges, and we are able to use the multisite electrode to deliver electrical stimuli that evoke multidirectional, graded abdominal motions in both pupae and adult moths. Finally, in loosely tethered flight, we have used stimulation through the flexible microelectrodes to alter the abdominal angle, thus causing the flying moth to deviate to the left or right of its intended path.**

***Index Terms*—Biomedical electrodes, insect, neuromuscular stimulation.**

I. Introduction

THERE is considerable interest in creating insect-based microair vehicles (i-MAVs) that would combine the advantageous features of insects—small size, effective energy storage, navigation ability—with the benefits of microelectromechanical system (MEMS) and electronics—sensing, actuation, and information processing. The two basic components of the i-MAV are the telemetry system and stimulation system, as shown in Fig. 1. The telemetry system provides a communication link between the insect and the base station, while the stimulation system interfaces with the nervous system of the insect to bias the insect's flight path. Several groups have developed telemetry systems that can be glued onto insects [1]–[3]. Our group has previously developed a wireless stimulation system for i-MAVs, which is light enough to be carried by the moth and is able to generate various voltage pulses for neural stimulation using tungsten wires [4].

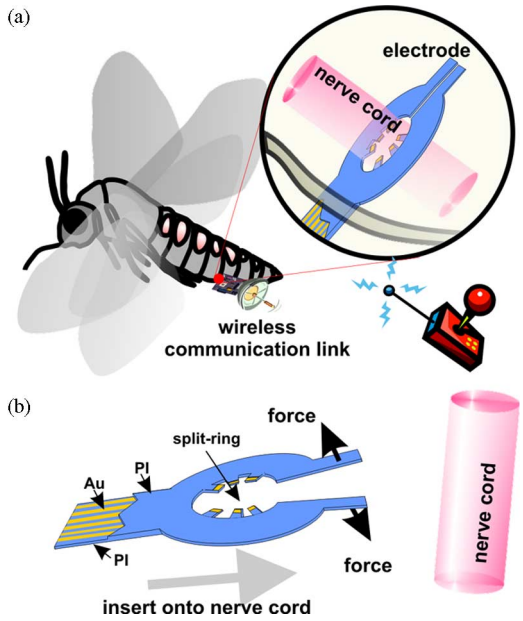

Fig. 1. (a) Conceptual illustration of insect-based i-MAVs. i-MAVs require a communication link to send and/or receive data and a bioelectronic interface, which is the focus of this manuscript. (b) Schematic of the FSE insertion process, showing how the split ring can be opened to fit around the nerve cord.

The other basic component of an i-MAV is the stimulation system. Various stimulation schemes, such as optical stimulation [5], muscle heating [6], drug injection [7], and electrical stimulation of the muscle and nervous systems [5], [8] have been proposed to bias the flight of the insect. Among these stimulation schemes, electrical stimulation is especially promising because of its low power consumption, ease of integration with electronics, and fast response time. Within the realm of electrical stimulation, direct stimulation of the insect's central nervous system (CNS) is likely to be more robust than stimulation of the musculature in real-world applications because CNS stimulation allows the insect's natural flight-control circuitry to process the applied inputs, thus minimally perturbing the insect's flight-control system and allowing the insect, for instance, to avoid

Manuscript received September 2, 2009; revised November 11, 2009 and January 8, 2010; accepted January 12, 2010. Date of publication February 18, 2010; date of current version June 16, 2010. This work was supported by the Defense Advanced Research Projects Agency Hybrid Insect Micro-Electro-Mechanical Systems Program. *Asterisk indicates corresponding author.*

W. M. Tsang is with the Research Laboratory of Electronics, Massachusetts Institute of Technology, Cambridge, MA 02139 USA (e-mail: wmtsang@mit.edu; wmtsang@alumni.cuhk.net).

A. L. Stone and J. G. Hildebrand are with the University of Arizona, Tucson, AZ 85721 USA (e-mail: alstone@u.arizona.edu; jgh@neurobio.arizona.edu).

Z. N. Aldworth and T. L. Daniel are with the University of Washington, Seattle, WA 98195 USA (e-mail: zna@u.washington.edu; danielt@u.washington.edu).

A. I. Akinwande is with the Department of Electrical Engineering and Computer Science Department, Massachusetts Institute of Technology, Cambridge, MA 02139 USA (e-mail: akinwand@mtl.mit.edu).

*J. Voldman is with the Electrical Engineering and Computer Science, Massachusetts Institute of Technology and the Research Laboratory of Electronics, Massachusetts Institute of Technology, Cambridge, MA 02139 USA (e-mail: voldman@mit.edu).

Color versions of one or more of the figures in this paper are available online at http://ieeexplore.ieee.org.

Digital Object Identifier 10.1109/TBME.2010.2041778

obstacles en route to a destination. Although direct CNS stimulation through a tight neural-electrode interface is preferable, most existing neural probes (such as insertion electrodes or cuff electrodes [9]) focus on applications for mammals, whose neural systems are significantly larger than those of insects. The small size and limited operating space of insects preclude direct application of these designs to insects.

Classically, insulated (except at the tip) thin metal wires [1]–[4] or hand-made clip electrodes [10] have been employed for neural studies on freely moving or loosely tethered insects. Although significant insights have been obtained using these electrodes, the number of stimulation sites, production efficiency, and reproducibility of these electrodes are intrinsically limited due to their manual nature. The advancement of MEMSs opens a window to multisite and consistently produced neural probes for small neural systems. 3-D shape-memory alloy microelectrodes [11] and silicon- or polymer-based flexible insertion microelectrodes [12], [13] have been used in insect applications. All of these electrodes, however, are designed for neural recording rather than stimulation. Moreover, they are difficult to implant and attach to the CNS of the insect because of the small size of the nerve cord in insects ($\sim$ few hundred micrometers in diameter), as well as the limited operating space within the insect cuticle.

Here, we introduce a flexible split-ring electrode (FSE) for insect flight biasing that uses electrodes arranged in a spoke-like manner to provide circumferential stimulation around an insect's ventral nerve cord. The electrodes are fabricated by standard MEMS processing, allowing for efficient large-scale production. We show that the electrodes can provide multisite electrical stimulation of the CNS of the moth *Manduca sexta* and that we are able, using a $\sim$20 min insertion procedure, to implant them into pupae as early as seven days before emergence of the adult moth without rejection of the implant or damage to the insect. We characterized the electrical properties of the FSE in saline solution *in vitro* and characterized the stimulation efficacy of the FSE *in vivo* in both pupae and adult moths. We demonstrated that stimulation with the FSE can elicit multidirectional graded abdominal motions in both pupae and adult moths, and these abdominal motions can cause ruddering to alter the flight path of the adult moth.

The hawkmoth, *Manduca sexta*, was chosen for this research for several reasons. These moths have been continuously reared in colonies for more than 20 years at our universities, and methods for surgery and implantation of electrodes are well established. The moth is commonly used in research, and much is known about its neurobiology, physiology, and flight-control mechanisms.

II. Methods

A. Electrode Fabrication and Packing

The FSE is composed of two layers of polyimide (PI) with gold sandwiched in between [see Fig. 1(b)]. We provide a detailed description of the FSE dimensions in Fig. 2. The main steps of fabrication are shown in Fig. 3. First, a 1.0-μm-thick aluminum layer, which acts as a sacrificial releasing layer, is

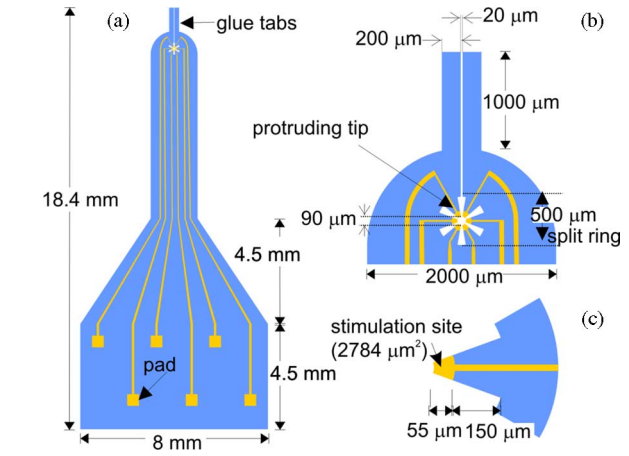

Fig. 2. FSE dimensions: (a) entire device; (b) split-ring region; (c) tip region.

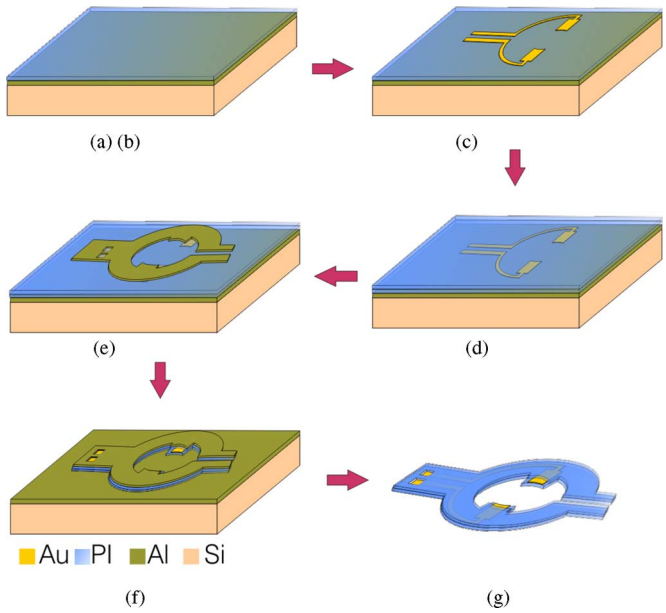

Fig. 3. Electrode fabrication process: (a) deposit Al as sacrificial layer; (b) coat and cure base PI layer; (c) deposit and pattern Ti/Au/Ti layer as the electrical conductive traces; (d) coat and cure top PI layer; (e) deposit and pattern Al layer as hard mask for dry etching; (f) pattern the FSE structure by O_2/CF_4 plasma etching; (g) release the FSE from the substrate by dissolving the sacrificial Al layer in HF.

evaporated onto a piranha-cleaned 150-mm silicon wafer using physical vapor deposition [see Fig. 3(a)]. A base layer of PI (HD 4110, HD Microsystem) is subsequently spun onto the wafer to yield a layer thickness of $\sim$15 μm. The base PI layer is then partially cured at 320 °C in N_2 for 0.5 h to provide a chemically and physically stable surface for the further processing while leaving some unterminated bonds for attaching the top PI layer [12] [see Fig. 3(b)].

The PI-coated wafers are then spin coated with a 1.5-μm-thick layer of photoresist (AZ 5214, Clariant). A negative image of the electrode traces is created using image-reversal photolithography. Electron-beam evaporation allows for the deposition of

a 10-nm-thick titanium adhesion layer followed by a 250-nm-thick gold conduction layer and finally a 20-nm-thick titanium protection layer onto the substrates, followed by liftoff in acetone [see Fig. 3(c)]. The top layer of the PI is spun onto the substrate using the same protocol as the base PI layer, and then the whole structure is fully cured at 360 °C in N_2 for 1 h to complete the imidization process, leaving the structure in its final state [see Fig. 3(d)]. The final structure is ∼16-μm thick owing to vertical shrinking of the PI layers during the curing process.

Next, we deposit and pattern a 0.5-μm-thick aluminum layer to be used as the hard mask for the final PI etch by e-beam and positive photolithography with wet etching, respectively [see Fig. 3(e)]. We define the shape of the electrode and open windows for the stimulation sites with an O_2/CF_4 plasma. During the etching process, the unwanted PI material is removed by the plasma, while the Au stimulation sites and the PI structure are protected by the top titanium protection layer and aluminum layers, respectively. The plasma-etching process is performed by an electron cyclotron resonance-enhanced reactive-ion etcher (gas flows of 70 sccm for O_2 and 15 sccm for CF_4, source power of 300 W and RF bias power of 50 W, with a chamber base pressure of 50 mTorr, resulting in a PI etch rate of ∼0.67 μm/min) [see Fig. 3(e)]. Finally, the electrode structures are released from the wafer substrate by dissolving the aluminum layers (hard mask and sacrificial layer) in a 0.5% hydrofluoric acid solution [see Fig. 3(f)].

To connect the devices for testing, we manually attach 1.5-m-long ultrathin stainless steel wires (50 μm in diameter and covered with Teflon, A-M Systems, Inc.) to the electrode pads using silver epoxy (CW2400, ITW Chemtronics). The connecting regions are further sealed with insulating epoxy (Scotch-Weld 2216 B/A, 3M), to enhance the mechanical attachment between the electrode and wires.

B. Electrode Implantation

Most FSE implantations are performed in stage-16 pupae, two days prior to adult moth emergence (eclosion). Animals are anesthetized in ice for 1–2 h, the pupal cuticle is removed, and an incision is made in the underlying adult cuticle at the position of the ventral fourth abdominal segment, just posterior to the folded developing wings (see Fig. 4). A glass probe is used to isolate the ventral nerve cord and position it for FSE insertion. The FSE is brought onto the nerve cord so that the glue tabs separate and the bundle of nervous tissue slides between them and into the split ring. Medical device adhesive (Loctite 3211, RS Hughes) is applied to the glue tabs and polymerized. The FSE is then positioned with the linked glue tabs extending below the nerve cord and the PI body of the FSE extending through the incision. A small amount of absorbable gelatin sponge (Pharmacia Gelfoam, Fisher Scientific) is placed into the incision on both sides of the FSE. The incision is closed using 3M Vetbond glue (Animart) with an outer layer of Loctite 4013 adhesive (RS Hughes). Moths are housed in incubators at 24 °C and 80% humidity and allowed to recover overnight prior to stimulation experiments.

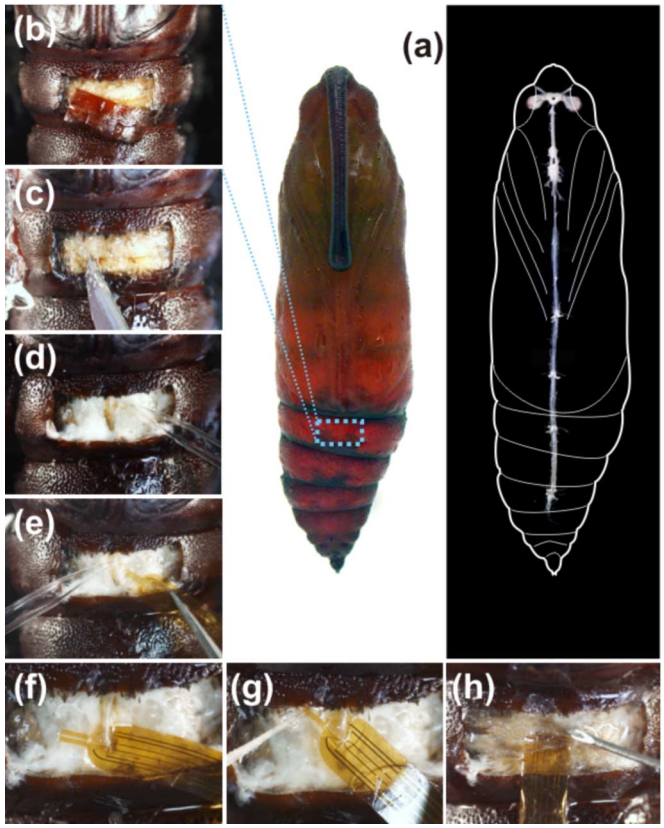

Fig. 4. Overview of device implantation surgery. (a) Electrode implantation site in pupa; (b) open window in pupal cuticle; (c) make incision in underlying adult cuticle; (d) isolate nerve cord on glass probe; (e–f) place split-ring portion of electrode onto the nerve cord; (g) add glue to the glue tabs and polymerize; (h) insert electrode into incision and seal using surgical glue.

C. Electrical Characterization

The charge-transport properties of the FSE were studied by electrochemical impedance spectroscopy (EIS) in phosphate buffered saline solution (PBS). The measurements were performed via a potentiostat (VersaSTAT3, Princeton Applied Research) with a microcell kit (Model K0264, Princeton Applied Research). The EIS measurements were performed using a two-electrode configuration with a Pt wire as the counter electrode. The measurements were taken between 1 Hz and 100 kHz, using a 10-mV ac signal and used to fit with an equivalent circuit model using Zview (Scribner Associates, Inc.).

D. Electrical Stimulation

Electrical stimulation experiments were performed on both stage-18 pupae (one day prior to emergence) and adult moths. A train of bipolar voltage pulses was applied across each of the 15 pairs of stimulation sites using an isolated pulse stimulator (Model 2100, A-M Systems, Inc). The duration of the individual voltage pulses and of the pulse train were fixed to 1 and 500 ms, respectively. The frequency and the magnitude of the voltage pulses varied in the ranges 50–333 Hz and 1–10 V, respectively. Moreover, the 1.5-m-long stainless steel wires (total six) were light enough not to hinder the moth's flight

behaviors and therefore allowed us to conduct loosely tethered flight-control experiments with the flying moth.

III. Results and Discussion

A. Electrode Design and Implantation

It is well known that insects maneuver their flight not only through rapid adjustments of their flapping wings, but also through dynamic control of their center of gravity [15]. They flex their abdomen to effect center-of-gravity shifts and consequently their flight attitude. Prior research has shown that stimulation of the ventral nerve cord of the moth with tungsten-wire electrodes elicits abdominal motions [16], presumably by activating motoneurons or interganglionic interneurons. The identity and functional characteristics of these neurons are still unclear. To ensure localized activation of axons, we designed the FSE to provide multisite stimulation circularly around the nerve cord of the moth. The procedure for insertion of the FSE is illustrated in Figs. 1 and 4 along with a detailed description of the FSE dimensions in Fig. 2. We determined the FSE dimensions based on anatomical measurements of the abdominal connective in the fourth abdominal segment in stage-16 pupae, which was found to be ~450 μm in diameter.

We initially developed FSE designs with four, six, or eight stimulation sites. We found that the four-site FSEs had insufficient multistimulatory capability to achieve multi-directional abdominal motion, while the eight-site FSEs required very small protruding tips (25 μm $\times$ 175 μm), which made the FSEs too delicate for electrode implantation. Hence, we adopted the six-site design for the experiments presented in this paper. Images of the fabricated FSEs are shown in Fig. 5. We chose to use PI for the FSE mechanical material due to its flexibility (Young's modulus: 3.5 GPa and elongation: 45%), biocompatibility, and thermal stability (during processing). Although PI is known to be able to absorb water, we did not observe any changes in performance due to water absorption [see Fig. 6(b)] nor did absorption affect fabrication. Moreover, PI is widely used for neural probes [8], [14], [17]. The split-ring design of the FSE allows us to split open the ring of the FSE during insertion [see Fig. 1(b)]. In addition, the protruding tips penetrate into the connective tissue surrounding the nerve cord after insertion of the FSE. Hence, the stimulation sites, which are located at the ends of the protruding tips, could directly stimulate the nerve cord. The two glue tabs at the head of the FSE acted as "handles" to manipulate the implant, and, after the FSE had been inserted on the nerve cord, we applied glue to the tabs to lock the FSE in place. We chose gold for the electrode metal even though its more limited charge-injection capability compared to other popular electrode materials (e.g., iridium oxide) results in a relatively high-stimulation voltage. This is because our focus here was on the development of the split-ring electrode geometry, and so we wanted to minimize fabrication complexity while using a biocompatible metal [17], [18]. Extension to other materials with higher charge-injection capability, such as platinum black, iridium oxide, or carbon nanotubes, is straightforward by coating with a postfabrication electroplating process.

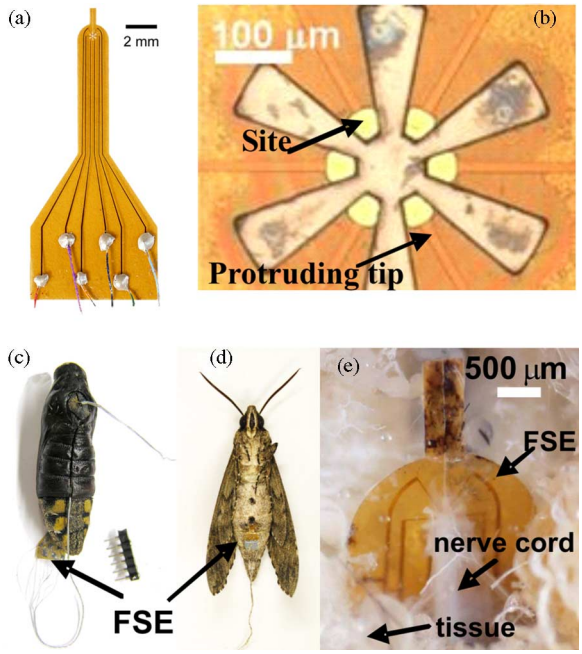

Fig. 5. (a) Image of the FSE with color-coded wire connections; (b) close-up image of the FSE at the split-ring region; (c) image of a pupa with inserted FSE; (d) eclosed adult moth with FSE inserted at the pupal stage; (e) image of dissected adult moth showing the growth of connective tissue around the FSE.

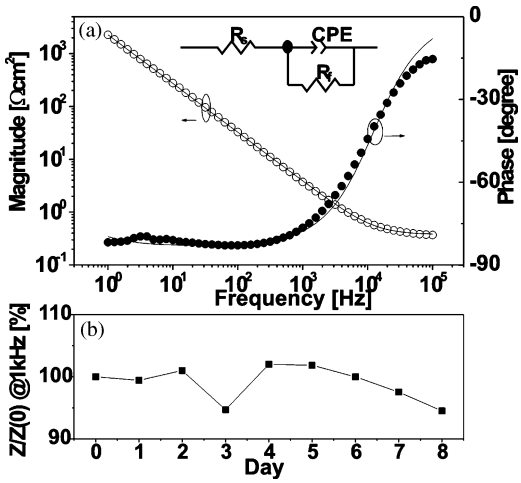

Fig. 6. (a) EIS spectra of a representative FSE in PBS (circles) along with the fit (lines) to the equivalent circuit model for charge conduction. (b) Variation of impedance of the FSE at biologically relevant frequency –1 kHz for immersed at PBS solution over a week.

We have been able to implant FSEs into adult moths as well as pupal stages 12–17 (7–2 days prior to eclosion), with the most successful pupal implantation surgery achieved in stage-16 pupae. Images of a pupa just after insertion of the FSE and after adult emergence are shown in Fig. 5(c) and (d), respectively. The total surgical time for the implantation was ~20 min, and the results are summarized in Table I. The successful eclosion rate of the pupae after FSE insertion was 75% to 94 %, depending on the stage of the pupa. Although the glue tabs provide some

TABLE I
SURGICAL RESULTS OF FSE INSERTION

	Eclosion	Nos.
Stage 12-13 Pupa	75%	8
Stage 14-15 Pupa	72%	39
Stage 16 -18 Pupa	94%	123

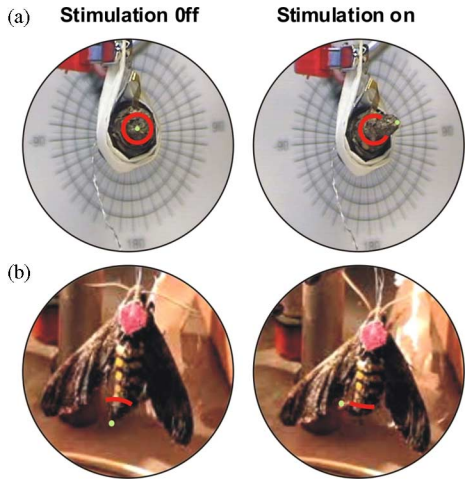

Fig. 7. Fully tethered abdominal stimulation: (a) images of a pupa as seen along the abdomen–thorax axis before and during electrical stimulation, showing that the tip of the abdomen (dot) moves with respect to the moth (circle), thus changing the abdominal angle. (b) Analogous stimulation of an adult.

stability to the implanted FSE, one advantage of implanting electrodes in pupae is the potential for tissue to grow around and onto the PI surface, further securing the FSE. Indeed, images of dissected adult moths with FSEs implanted in stage-16 pupae show growth of connective tissue around the FSE PI and within the split-ring portion of the FSE (see Fig. 5). This new growth of peri-implant tissue appears to be derived from the dorsal pad, a thick band of connective tissue attached to the nerve cord.

B. Electrical Characterization

Prior to *in vivo* characterization of the FSE in the moths, the electrical connections between the FSE and the manually assembled wires were verified by EIS measurement in saline solution. Moreover, the charge-injection capability and the ion-transport conductivity of the electrode are proportional to the interface capacitance between the electrode and the solution, which could be estimated from the EIS spectrum with an equivalent circuit model. The EIS spectrum of a representative FSE is shown in Fig. 6 along with a standard equivalent-circuit model for the electrode. In the model, the interface between the FSE and PBS is represented by a constant phase element (CPE, with impedance $Z_{dl} = 1/C_{dl}(j\omega)^n$) in parallel with the Faradic impedance R_f, while R_s is the spreading resistance of the solution. The fitted values of R_s, R_f, and C_{dl} are 4.3 kΩ, 5.5 GΩ, and 68 μF$\cdot$s^{n-1}/cm^2, respectively. The value of *n* is determined to be 0.92, which is close to the value of 1 for an ideal capacitor and the value of C_{dl}(68 μF$\cdot$s^{n-1}/cm^2) is similar to the reported value (72 μF$\cdot$s^{n-1}/cm^2) of gold wire (area: 5×10^4 μm^2) [19]. This suggests that the interface between the FSE and the solution can be accurately represented by a polarizing charge double layer at the electrode–electrolyte interface and implies that the charge transfer of the FSE is attributed to charge injection at the stimulation sites rather than current leakage from the interface of the top and base PI layers.

As it is well known that the PI can absorb water, which could in turn alters its properties, we studied the long-term electrical stability of the FSE in saline. We did not observe any significant change in the electrical properties of the FSE after it was immersed in saline over a week. The variation of impedance of the FSE at the biologically relevant frequency of 1 kHz is less than 10% after a week of immersion, as shown in Fig. 6(b). The lifespan of the adult moth is typically around a week; therefore, these results suggest that the FSE is stable enough for our application.

C. Electrical Stimulation

To demonstrate the stimulation functionality of the FSEs, we first used them to evoke abdominal motions of pupae and adult moths in fully tethered preparations (see Fig. 7). A total of ten pupae and ten adult moths were employed in the experiments; four of the pupae and adults were the same individuals at different developmental stages. We assigned the abdominal responses of the animals to eight distinct directions, and the statistical results are shown in Fig. 8(a) and (b) for the pupae and adult moths, respectively. Moreover, to investigate whether responses to stimulation were variable across developmental stages, we also measured abdominal flexion in fully tethered preparations of the same animal at pupal and adult stages [see Fig. 8(c) and (d)]. Stimulation through the FSE could elicit multidirectional abdominal movements in both pupae and adult moths. As anticipated from prior research [16], the directions of abdominal movement depended on the specific electrode sites selected for stimulation. The six-site FSEs contain 15 possible stimulation site pairs, in all animals at least two (and as many as six) distinct abdominal movements were observed in response to stimulation of the various electrode combinations. The elicited movements of the pupal abdomen were predominantly dorsolateral [see Fig. 8(a)], whereas those in adult moths [see Fig. 8(b)] were mainly ventral.

Interestingly, although the responses of animals were individually repeatable at a single developmental stage, the responses differed between animals and changed as the animal developed from pupa to adult. In one example in which the responses to FSE stimulation were compared in pupa and adult [see Fig. 8(c)–(d)], stimulation site pair (5, 6) evoked abdominal flexion to the right at the pupal stage, but stimulation through the same

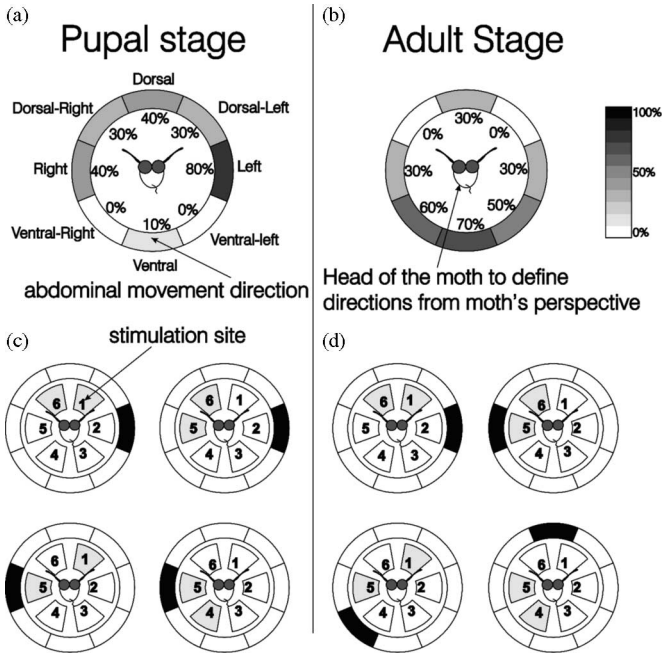

Fig. 8. Variation of stimulation with developmental stage. The statistical distribution of the directions of stimulated abdominal response (illustration of moth head) on the (a) pupae and (b) adult moths with the FSE stimulation. The outer ring signifies the resulting direction of abdominal flexion, while the color gradation indicates the percentage of animals that had motion in the specified direction due to stimulation, using any combination of electrodes. For example 80% of pupae had at least one electrode combination that would elicit motion to the left, while 70% of adults had at least one electrode combination that would elicit motion to ventral. In (c) and (d), the abdominal responses of a particular moth with respect to four distinct pairs of the stimulation sites at its pupal and adult stage are reported. The inner ring depicts the stimulation sites (labeled with number) with respect to the axis of the animal (illustration of moth head). For example, stimulation site pair (5, 6) evoked abdominal flexion to the left at the pupal stage and stimulation through the same pair elicited abdominal flexion to the right in the adult.

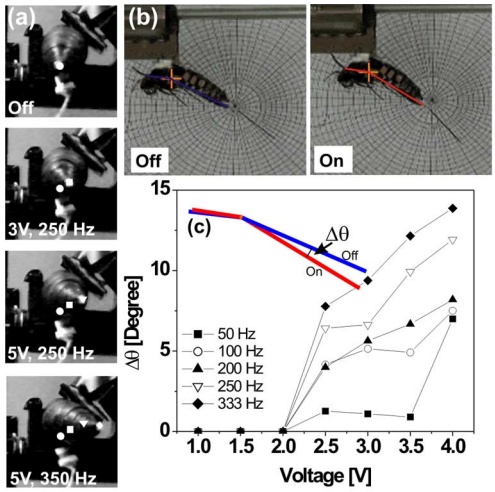

Fig. 9. The magnitude of the abdominal flexion with respect to the magnitude and the frequency of the stimulation signal: (a) image of the pupa without and with FSE stimulation. The tip of the abdomen was labeled by (•), (■), (◆), and (▼) for the stimulation signal of (0 V), (3 V, 250 Hz), (5 V 250 Hz), and (5 V, 350 Hz) using FSE sites (3,5), respectively. (b) Image of the adult moth without and with FSE stimulation. (c) Dependence of the abdominal flexion angle against the magnitude and the frequency of the stimulation signal; insert shows the definition of the abdominal flexion angle.

pair elicited abdominal flexion to the left in the adult. Such differences among experiments might reflect variation in the orientation of electrodes relative to the nerve cord in different preparations, movement after implantation, or anatomical variability among insects. The differences between pupal and adult responses likewise might be due to movement of the FSE but probably also reflect developmental differences in the location and identity of axons in the nerve cord and changes in the mechanical articulation of the abdomen [19]. On the other hand, the responses to FSE stimulation for each individual animal were repeatable for successive stimulations (>10) and were consistent at various time periods within a single developmental stage (e.g., day 1 and day 4 of the adult moth) (data not shown).

Generally, we observe an increment in the magnitude of the abdominal movements of the pupae and adult moths for increases in either voltage magnitude or pulse frequency of the stimulation signal, as shown in Fig. 9. In addition to the multidirectional abdominal movements, these graded abdominal movements are also needed to bias the moth's flight path smoothly. Therefore, we have investigated quantitatively the change of abdominal flexion angle of adult moths versus the magnitude and the frequency of the stimulation signal [see Fig. 9(b)–(c)]. The wings of an adult moth were removed to permit clear observation of abdominal flexion. The stimulation signal was applied to site pair (1, 2) of the FSE, resulting in abdominal flexion in the dorsal/ventral plane. For this particular moth, the threshold voltage to elicit abdominal movement was ∼2.5 V. The flexion angle increased with increasing magnitude or frequency of the voltage pulses. To interpret these results, we see from the EIS spectrum of the FSE (see Fig. 6) that the impedance of the FSE decreases with increasing frequency. Hence, increases in either voltage magnitude or pulse frequency imply an increase in stimulation current (for a voltage-controlled system). The stronger abdominal motion evoked at high-frequency/voltage levels is presumably due to the higher stimulation current exciting more axons in the nerve cord, which would in turn recruit more abdominal muscle fibers, though this hypothesis must be tested directly.

In flight-control experiments, we used the FSE to control abdominal ruddering in a loosely tethered forward-flying moth leading to a change in flight direction. As shown in Fig. 10, we were able to cause the flying moth to perform left and right turns following FSE stimulation. A total of seven loosely tethered moths were employed in the experiments; more than 70% (5/7) of them showed individually consistent turning motions during the flight with the repeated and successive FSE stimulations. Hence, these experiments indicate a good correlation between flight motions of the moth and the FSE stimulations. Although, these results are preliminary, they demonstrate the ability of the pupa-implanted FSE to alter the trajectory of a flying moth and are a significant step toward the i-MAVs application. Together, our results demonstrate the ability to robustly implant electrical stimulation devices into moths and subsequently perform multisite stimulation that evokes behavioral responses. These

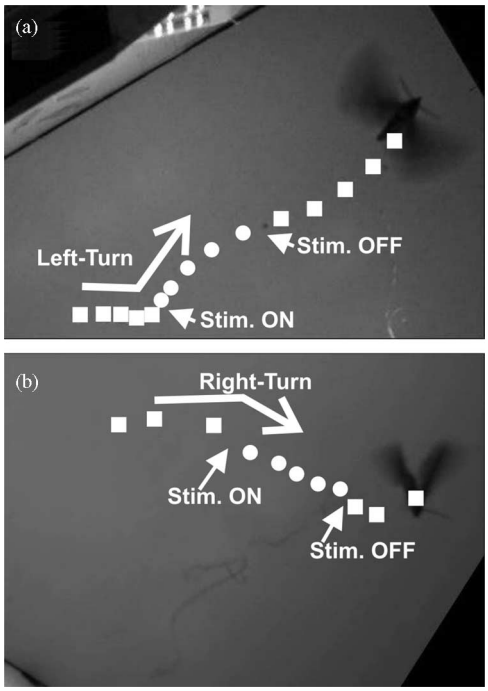

Fig. 10. Images showing the loosely tethered moth as it performs (a) left and (b) right turns, following stimulation using FSE sites (4, 6) and (5, 6), respectively.

techniques and technology set the stage for the ability to both stimulate and, presumably, record from the nervous systems of freely moving insects, providing new understanding of insect neurophysiology in more natural environments.

IV. Conclusion

Neural probes for insect applications are constrained by difficulties relating to the minimization of existing mammal-based microelectrodes and the small size of the insect's nervous system. Here, we present an FSE for insect flight control, using multisite stimulation around the nerve cord of the moth *Manduca sexta*. To our knowledge, this is the first microfabricated neural probe for electrical stimulation of an insect's CNS. We demonstrate that the FSE is able to stimulate multidirectional (by changing stimulation sites) and graded (by altering voltage or frequency) abdominal movements in both pupae and adult moths. Using abdominal flexion/ruddering, we were able to cause flying moths to perform right and left turns. Future work will focus on improving the design of the FSE to achieve consistent results across animals and to optimize the stimulation properties of the FSE by employing alternative materials and geometries for the stimulation sites.

Acknowledgment

The authors would like to thank the Microsystems Technology Laboratories for fabrication assistance. They would also like to thank Dr. Levine for research expertise and editing of the manuscript, S. Mackzum, M. Marez, and B. Nyugen for care and rearing of *Manduca sexta* moths, and S. Murray for assistance with flexible split-ring electrode characterization.

References

[1] H. Fischer, H. Kautz, and W. Kutsch, "A radiotelemetric 2-channel unit for transmission of muscle potentials during free flight of the desert locust, *Schistocerca gregaria*," *J. Neurosci. Methods*, vol. 64, pp. 39–45, 1996.

[2] P. Mohseni, K. Nagarajan, B. Ziaie, K. Najafi, and S. B. Crary, "An ultralight biotelemetry backpack for recording EMG signals in moths," *IEEE Trans. Biomed. Eng.*, vol. 48, no. 6, pp. 734–737, Jun. 2001.

[3] N. Ando, I. Shimoyama, and R. Kanzaki, "A dual-channel FM transmitter for acquisition of flight muscle activities from the freely flying hawkmoth, *Agrius convolvuli*," *J. Neurosci. Methods*, vol. 115, pp. 181–187, 2002.

[4] D. C. Daly, P. P. Mercier, M. Bhardwaj, A. L. Stone, J. Voldman, R. Levine, J. G. Hildebrand, and A. P. Chandrakasan, "A pulsed Uwb receiver Soc for insect motion control," in *Proc. ISSCC 2009*, pp. 200–201.

[5] H. Sato, C. W. Berry, B. E. Casey, G. Lavella, Y. Yao, J. M. V. Brooks, and M. M. Maharbiz, "A cyborg beetle: Insect flight control through an implantable, tetherless microsystem," in *Proc. 21st IEEE Int. Conf. Micro Electro Mech. Syst. (MEMS 2008)*, pp. 164–167.

[6] A. Bozkurt, A. Lal, and R. Gilmour, "Electrical endogenous heating of insect muscles for flight control," in *Proc. 30th Int. Conf. IEEE Eng. Med. Biol. Soc. (EMBS 2008)*, pp. 5786–5789.

[7] A. J. Chung and D. Erickson, "Engineering insect flight metabolics using immature stage implanted microfluidics," *Lab Chip*, vol. 9, pp. 669–676, 2009.

[8] A. Bozkurt, R. Gilmour, D. Stern, and A. Lal, "MEMS based bioelectronic neuromuscular interfaces for insect cyborg flight control," in *Proc. 21st IEEE Int. Conf. Micro Electro Mech. Syst. (MEMS 2008)*, pp. 160–163.

[9] P. Heiduschka and S. Thanos, "Implantable bioelectronic interfaces for lost nerve functions," *Prog. Neurobiol.*, vol. 55, pp. 433–461, 1998.

[10] S. Ye, J. P. Dowd, and C. M. Comer, "A motion tracking system for simultaneous recording of rapid locomotion and neural activity from an insect," *J. Neurosci. Methods*, vol. 60, pp. 199–210, 1995.

[11] S. Takeuchi and I. Shimoyama, "A three-dimensional shape memory alloy microelectrode with clipping structure for insect neural recording," *J. Microelectromech. Syst.*, vol. 9, pp. 24–31, 2000.

[12] D. R. Lemmerhirt, E. M. Staudacher, and K. D. Wise, "A multitransducer microsystem for insect monitoring and control," *IEEE Trans. Biomed. Eng.*, vol. 53, no. 10, pp. 2084–2091, Oct. 2006.

[13] J. R. Gray, V. Pawlowski, and M. A. Willis, "A method for recording behavior and multineuronal CNS activity from tethered insects flying in virtual space," *J. Neurosci. Methods*, vol. 120, pp. 211–223, 2002.

[14] P. J. Rousche, D. S. Pellinen, D. P. Pivin, J. C. Williams, R. J. Vetter, and D. R. Kipke, "Flexible polyimide-based intracortical electrode arrays with bioactive capability," *IEEE Trans. Biomed. Eng.*, vol. 48, no. 3, pp. 361–371, Mar. 2001.

[15] C. P. Ellington, "The aerodynamics of hovering insect flight," *Philos. Trans. R. Soc. Lond., B. Biol. Sci.*, vol. 305, pp. 1–181, 1984.

[16] M. R. Enstom, J. K. Longnion, T. L. Daniel, M. S. Tu, C. Diorio, and M. A. Willis, "Abdominal ruddering and the control of flight in the hawkmoth," presented at *The Society Integrative and Comparative Biology Meeting*, Toronto, 2003.

[17] L. A. Geddes and R. Roeder, "Criteria for the selection of materials for implanted electrodes," *Ann. Biomed. Eng.*, vol. 31, pp. 879–890, 2003.

[18] G. Voskerician, R. S. Shawgo, P. A. Hiltner, J. M. Anderson, M. J. Cima, and R. Langer, "*In vivo* inflammatory and wound healing effects of gold electrode voltammetry for MEMS micro-reservoir drug delivery device," *IEEE Trans. Biomed. Eng.*, vol. 51, no. 4, pp. 627–635, Apr. 2004.

[19] E. T. McAdams, J. Jossinet, R. Subramanian, and R. G. E. McCauley, "Characterization of gold electrodes in phosphate buffered saline solution by impedance and noise measurements for biological applications," in *Proc. 28th IEEE EMBS Annu. Int. Conf.*, 2006, pp. 4594–4597.

[20] R. B. Levine and J. W. Truman, "Dendritic reorganization of abdominal motoneurons during metamorphosis of the Moth, *Manduca sexta*," *J. Neurosci.*, vol. 5, pp. 2424–2431, 1985.

Wei Mong Tsang (M'10) received the B.Eng. (first class Honors) and M.Phil. degrees in electronic engineering from the Chinese University of Hong Kong, Hong Kong, in 2000 and 2002, respectively, and the Ph.D. degree in electrical and electronic engineering from the University of Surrey, Guildford, U.K., in 2007.

He is currently a Postdoctoral Associate in the Research Laboratory of Electronic, Massachusetts Institute of Technology, Cambridge. His research interests include the bio-microelectromechanical systems, neural prosthetics, electron field emission, and nanotechnology.

Dr. Tsang is a member of the Materials Research Society. He was the recipient of E. W. Müller "Outstanding Young Scientist Award" from the International Field Emission Society in 2006.

Alice L. Stone received the B.S. degree (Honors) in biology from the University of Michigan, Ann Arbor, in 1985.

She is currently with the University of Arizona, Tucson, where she is engaged in research on immunoparasitology, tissue engineering, neurobiology, microdissection and animal surgery, cell culture, histology, immunohistochemistry, protein analysis, and imaging of biological samples via light, fluorescent and electron microscopy. She is the author or coauthor of nine scientific papers published in veterinary pathology and biomedical engineering journals.

Ms. Stone was the recipient of the Edmund A. Arbas Award from the Arizona Research Laboratories, University of Arizona, in April 2009.

Zane N. Aldworth received the B.S. degree in physics from the University of Puget Sound, Tacoma, WA, in 1998, the B.S. degree in biology and the Ph.D. degree in neuroscience from Montana State University, Bozeman, in 1999 and 2007, respectively.

He is currently a Research Associate at the Biology Department, University of Washington, Seattle. His research interests include neural coding, neural ethology, and structure–function relations in neural systems.

Dr. Aldworth is an active member in the Society for Neuroscience and the Society of Integrative and Comparative Biology. He was the recipient of the Phil Kopriva Graduate Fellowship and the Gary K. Lynch Memorial Award.

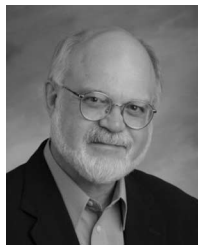

John G. Hildebrand received the Ph.D. degree in biochemistry from Rockefeller University, New York, in 1969.

He is currently a Regents Professor and the Head of the Department of Neuroscience, University of Arizona, Tucson, where he is engaged in research on insect nervous systems and behavior.

Prof. Hildebrand is a member of the National Academy of Sciences, American Academy of Arts and Sciences, and German Academy of Sciences "Leopoldina;" a foreign member of the Norwegian Academy of Science and Letters; and a Fellow of the American Association for the Advancement of Science, Entomological Society of America, and Royal Entomological Society. He is also a Past President of several scientific societies and a frequent consultant to federal agencies, private foundations, and companies.

Tom L. Daniel, photograph and biography not available at the time of publication.

Akintunde Ibitayo Akinwande (F'08) photograph and biography not available at the time of publication.

Joel Voldman (S'92–M'02) received the B.S. degree in electrical engineering from the University of Massachusetts, Amherst, in 1995, and the M.S. and Ph.D. degrees in electrical engineering from the Massachusetts Institute of Technology (MIT), Cambridge, in 1997 and 2001, respectively.

He was a Postdoctoral Associate at Harvard Medical School, where he studied developmental biology. Since 2002, he has been with MIT, where he is currently an Associate Professor at the Department of Electrical Engineering and Computer Science. His research interests include microscale manipulation of cells for cell sorting, dielectric cell analysis, and stem cell biology, as well as electrode development for neurobiology.

Dr. Voldman is a member of the Technical Program Committee for the microTAS conference, and has been a member of the Transducers, IEEE Microelectromechanical Systems, and International Society for Stem Cell Research Program Committees. He was the recipient of several awards, including the National Science Foundation CAREER Award and the American Chemical Society Young Innovator Award.